14th CIRP Conference on Modeling of Machining Operations (CIRP CMMO)

Simulation of roughness and surface texture evolution at macroscopic scale during cylinder honing process

B. Goeldel [a]*, M. El Mansori [a], D. Dumur [b]

[a]*Arts & Métiers Paris Tech, LMPF, EA 4106, Rue Saint Dominique BP 508, 51006 Châlons-en-Champagne, France*
Supélec, Département Automatique, Plateau de Moulon, 3 rue Joliot-Curie, F 91192 Gif sur Yvette cedex, France
* Corresponding author. Tel.: +33 326 699 176; fax: +33 326 699 197.*E-mail address*: benoit.goeldel@ensam.eu.

Abstract

The honing process produces surface liners with specific functional properties. Engine performances and life expectancy are directly impacted by the quality of honed surface. The form quality, the roughness and the surface appearance manufactured by honing determine the friction of the piston in the liner. The process is however mechanically complex and the selection of the process parameters is currently based on empirical methods. The aim of this paper is thus to develop a macroscopic simulation environment which will help end-users during this setting-up stage. The development of this virtual tool is based on a space-time discretization and a macroscopic cutting model taking into account local contacts between the workpiece and the abrasive stones. The space-time discretization allows representing the machine environment including the tool, the workpiece and the machine kinematics. The cutting model allows converting kinematics and abrasive contacts in dynamic data and material removal rate by calculation. The cutting model is initially adjusted based on simple experiments. The stock removal equation is then extrapolated to the whole range of stone cutting conditions. This approximation allows simulating the real process and a whole honing cycle. Results are validated by comparison with industrial context experiments. The simulation of the whole honing cycle allows predicting the form quality, one of the roughness criteria and the surface appearance. Moreover, simulation results are represented by means of maps that allow looking at quality criteria for each point of the surface.

Selection and peer-review under responsibility of The International Scientific Committee of the "14th CIRP Conference on Modeling of Machining Operations" in the person of the Conference Chair Prof. Luca Settineri

Keywords: Honing; Grinding; Simulation.

Introduction

The optimization of honing for mass production of cylinder blocks is a major challenge for designers of internal combustion engines. The energetic performance of the engine depends partly on this operation. Honing allows modifying the topography of the contact surface between the cylinder and the piston segments [1]. The essential role of the interface is to ensure lubrication of the piston slides and the tightness of the combustion chamber. This strategy, which aims at reducing metallic contact, also allows oil consumption [2] and greenhouse gas emissions to be reduced, and the engine's life to be increased. Currently, the setting method of the surface creation process is based on empirical knowledge concerning abrasion [3]. It is complicated and costly in terms of time and equipment. Some models allow calculating the cutting force [4] for a stone. Other studies model the creation of grooves by some grit [5]. Certain studies [6], [7] simulate the vibratory behavior of the tool system. The goal of the current research is to endeavor to model honing abrasion in order to predict the quality of the surface obtained according to process parameters. The originality of the developed software is based on a linear model of the bearing ratio curve. Detailed analysis of this model has enabled us to predict the material removed, as well as the aspect of the honed surface (exact measurements, roughness, and texture). Experimental results, some coming from industrial series, validate our models and highlight certain unique honing properties. Finally, the characteristics of the final surface texture, which are the result of the study of simulated grooves, allow predicting surface aspect criteria.

1. The honing machine

The stones fixed on the honing tool are activated on 3 axes: a rotation *ω(t)*, an axial translation *z(t)* and a radial expansion *r(t)*. This axial expansion aimed at applying the stones to the surface of the cylinder bore can be conducted according to position, using a position control with an electromechanical activator (*EM*), or through pressure using a hydraulic jack (*HY*).

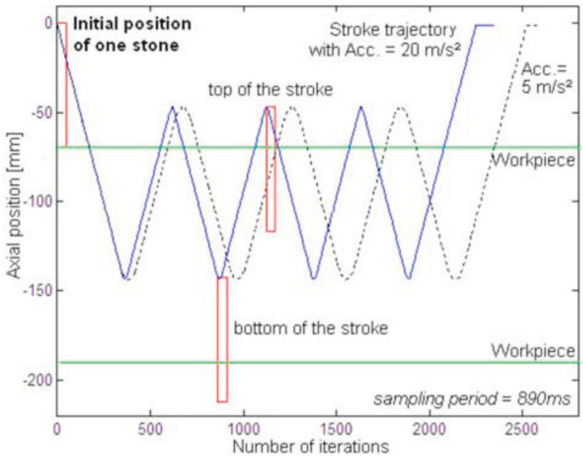

Fig. 1. Axial stroke trajectory

In normal honing, honing rotation speed *ω(t)* is constant and axial translation is carried out at constant alternate speed, forming a stroke motion (figure 1). The length of the stroke motion is calculated so that the honing tool overlaps the height of the stones by a third at their highest and lowest inversion points. The groove angle *α* and the cutting speed of the abrasive *Vc* are fixed to obtain the right texture and the best performance of the process [8]. For the linear part of the movement, the peripheral speed *Vp* and the stroke speed *Vb* are calculated to fulfill the honing angle *α*:

$$\tan\left(\frac{\alpha}{2}\right) = \frac{Vb}{Vp} \quad \text{and} \quad Vc = \sqrt{Vb^2 + Vp^2} \qquad (1)$$

As the honing tool mass is considerable, every reversal of direction is carried out at a controlled acceleration. In mass production, acceleration is set between 10 and 20m/s². Figure 1 illustrates the deterioration of the trajectory if it goes down to 5 m/s². A parabolic trajectory in stroke inversion, which may cause some defects on the honed surface, can be observed. Expansion of the stones is synchronized with the stroke motion and controlled by real time measurement of the diameter of the honed cylinder bore. These measurements are carried out via pneumatic nozzle fixed on the honing tool [9]. All of these elements will be considered during the simulation. The choice of abrasive is not the object of the simulation although it contributes to the quality of the resulting surface.

2. Simulation

2.1. Discretization

Studies of 3D modeling of cylinder bores have already been proposed [10]. They allow studying the constraints on the honed cylinder bores, their deformation, but they are unable to model the amount of material removed to the same extent. Microscopic abrasion studies [11], [12] are often limited to the study of the impact of a few abrasive particles and their results cannot really be applied to honing stones. Moreover, the influence of complex kinematics has never been studied. The proposed software is based on a surface representation of contact elements with square meshes of 1×1 mm. The kinematics of the motion and of the honing tool is simulated in detail [13]. Each of these meshes are linked to macroscopic criteria (shape, thickness, pressure), to microscopic criteria (roughness) and to mesoscopic criteria (aspect, texture). In spite of the evolution in the diameter of the cylinder bore and of the honing tool (by several hundreds of µm) during the honing process, the surface of the meshes is considered constant. The cylinder bore and the honing tool are therefore represented by matrices which have the same number of columns with a different number of lines (cylinder bore = remaining material; honing tool = stone thickness). Given the relative motion of the honing tool in relation to the cylinder bore, a time-domain discretization given by formula (2) allows obtaining at each iteration a single motion of a line or column.

$$\Delta t = \min\left(\frac{\Delta x}{Vp} \quad \frac{\Delta x}{Vb}\right) \qquad (2)$$

An overlaying model allows one to detect the cylinder bore meshes likely to be in contact with the honing stones at each iteration and subsequently to calculate their interaction and to determine the values of the "in-process measurements".

2.2. Kinematics and expansion

The evolution of the honing tool position in relation to the cylinder bore for a conventional honing machine is simulated in figure 1. The software also allows creating any motion *z(t)* linked to any given rotation speed *ω(t)* and expansion *r(t)* in real time.

If the expansion is controlled in position (electromechanical system *EM*), the position evolves in a linear way with an expansion speed *Vexp* programmed according to the stones contact expansion position. It is possible to impose a stronger impact. Once the expansion reaches an imposed residual material thickness, it remains constant during a number of additional strokes *Nbsup*, which can be programmed to carry out the “polishing stage”, aimed at refining the roughness. Honing with two different expansion speeds is also planned.

2.3. Roughness, stock removal and cutting force for electromechanical expansion

Roughness is one of the most important properties, which quantifies the quality of the honed cylinder bore. It is usually measured according to criteria which result from the bearing ratio curve (Figure 2 (a)) and must respect specific norms [14]. As in [15], it has been decided to represent this curve as a straight line, which will be defined entirely by 2 points *Fmin* and *Fmax*. The maximum roughness of a surface constitutes the distance measured on a perpendicular level between the deepest groove in the micro geometry and the most protuberant peak on the surface.

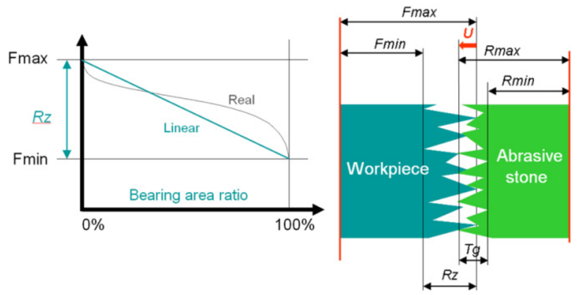

Fig. 2. Roughness modeling (a) Bearing ratio curve (b) Maximum roughness

The linear model of the bearing ratio contains this information. Figure 2 (b) represents these notions for the cylinder bore and the honing tool with:

$$Rz = Fmax - Fmin \text{ and } Tg = Rmax - Rmin \qquad (3)$$

Rz represents the roughness of the cylinder bore and *Tg* models the indentations of the stone particles. In order to study the interaction between the abrasive and the cylinder bore, consider the contact of one single honing mesh with a cylinder bore mesh and denote *U* the depth of penetration of the honing tool into the cylinder bore material. 8 different cases of penetration according to the respective values of *U*, *Tg* and *Rz* have to be examined. Figure 2 (b) represents case A1 for which $U<Tg<Rz$. Figure 3 (a) presents the overlap of the bearing ratios for this case. Thus consider a reference (Ox) linked to the honing tool, originating from *Rmin* and turned towards the cylinder bore. In this base, the rate of presence of honing tool abrasive particles and the bearing ratio of the cylinder bore are expressed as follows:

$$T\%_R(x) = \frac{Tg - x}{Tg} \text{ and } T\%_F(x) = \frac{x - Tg + U}{Rz} \qquad (4)$$

During the honing tool’s trajectory onto non-eroded zones, the bearing ratio remains unchanged. If one makes the assumption that the honing tool is extremely resistant and that it cannot be eroded; only the bearing ratio of the cylinder bore is affected.

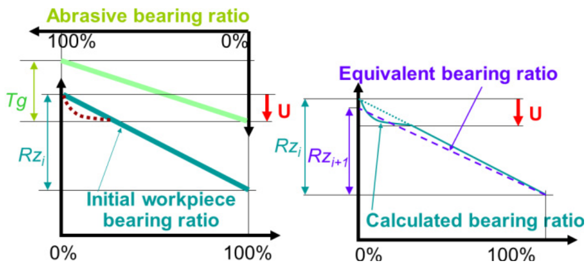

Fig. 3. Modification of the roughness profile (a) Superpositioning (b) New bearing ratio

In the interaction zone, the new bearing ratio of the cylinder bore is as follows on the high part:

$$T\%_F^{new}(x) = T\%_F(x) \times (1 - T\%_R(x)) \qquad (5)$$

The new bearing ratio is parabolic in the high zone (figure 3 (b)). This calculated bearing ratio is not linear in whole roughness thickness range. The equivalent linear bearing replaces the previous. The equivalent roughness Rz_{i+1} is calculated to respect the quantity of material removed, as in the following equation:

$$\int_0^{Rz_i} T\%_F^{new}(x) \cdot dx = \int_0^{Rz_{i+1}} \frac{x}{Rz_{i+1}} \cdot dx \qquad (6)$$

(1)

The minimum and maximum radial thicknesses of cylinder bore material are therefore updated using the following recurrence:

$$Fmin_{i+1} = Fmin_i \qquad (7)$$

$$Fmax_{i+1} = Fmax_i - \frac{U^3}{3 \cdot Tg \cdot (Fmax_i - Fmin_i)} \qquad (8)$$

According to our roughness model, the proportion of bearing surface in contact, for a radial position *x*, is written as follows:

$$S\%(x) = T\%_F(x) \times T\%_R(x) \tag{9}$$

The strength of contact of a mesh will be proportional to the quantity of material in contact along the entire thickness of the interaction zone. This is therefore given by:

$$\Gamma_c = \oint_{Contact} S\%(x) \cdot dx \tag{10}$$

In case A1, one obtains:

$$\Gamma_c^{A1} = \frac{U^3}{Tg \cdot Rz_i} \tag{11}$$

Similar formulations giving *Fmin*, *Fmax* and *Γc* are established for each case and are incorporated in the simulation. It is important to note that if *U* is higher than *Rz*, *Fmin* will also be reduced during the iterations and that all the *Γc* constitute a continuous but markedly non-linear curve according to *U*.

2.4. Texture, surface aspect

It is expected that as each stone motion leads to material removal; it leaves a trace on the honed surface. This trace is characterized by its direction, its relative depth quantified by *U* and by its absolute depth given by *Fmin* on the cylinder bore indicator.

During the honing cycle, these three variables have been recorded for all the traces. Further to simulation of the cycle, only visible traces for which *Fmin* is positioned between the final *Fmax* and *Fmin* are selected and compiled. Subsequently, the compilation of grooves is analyzed to establish the following criteria.

The first criterion is the number of visible traces, or groove density [16]. *(1)*

The ratio of orientation of the grooves, which corresponds to the “balance“ defined by [17], is calculated by dividing the number of visible rising traces by the number of visible traces. A good surface texture is composed of half rising grooves and half descending grooves [18]. To obtain a suitable texture, the angles of the visible traces must be close to the set angle *α*/2 with a tolerance of *Δα*. The conformity of the texture angle is expressed by the ratio of the number of visible traces with a right angle, over the total number of visible traces.

3. Simulation results and experimental validation

By measuring the micro geometry of the surface of the abrasive stones, the value of the indentation of the abrasive particles *Tg* has been determined for 2 types of regularly used stones: for IAS65/100, *Tg*=40 µm and SC500 *Tg*=20µm. This value is calculated as the maximum roughness observed with the tactile profilometer along a 16mm measure.

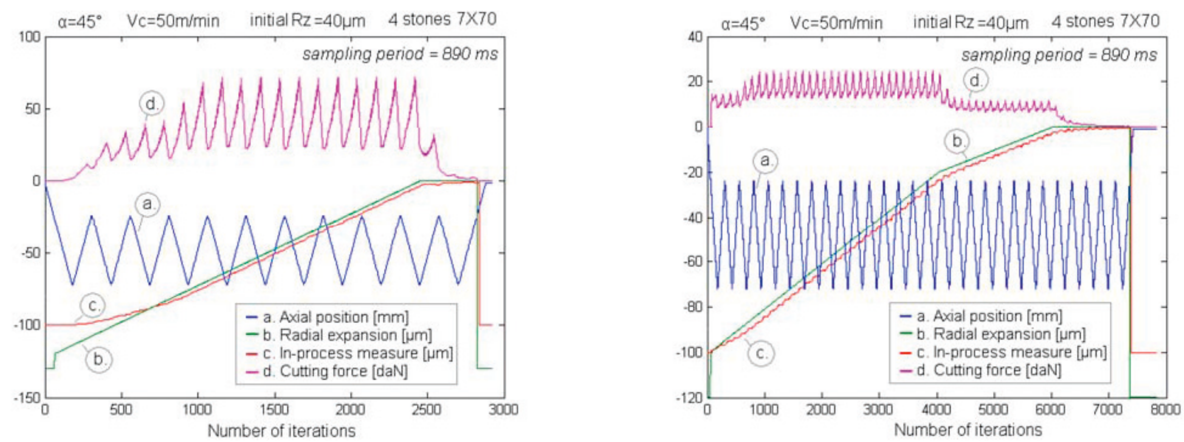

Fig. 4. Evolution of trajectory, cutting diameter and force with abrasive stones IAS65/100, (a) Single expansion speed: type 1 cycle (b) Double expansion speed: type 2 cycle

3.1. Simulated honing cycles

A cycle generator identical to those existing in industrial honing machines was installed. Figure 4 (a) presents type 1 honing: expansion starts on the −120µm radial position when the honing tool has begun into the cylinder bore to 2/3rds. Initially, little power can be observed because the abrasive stone only affects the ridges of the roughness profile of the contact surface. From the 900th iteration, expansion is equal to *Fmin* and the abrasive particles reach full material. In this case, the stabilized abrasion speed creates maximum force until the expansion ceases. On iteration 2400, the final measurement is reached and triggers the end of expansion. Subsequently, expansion is maintained in operation during the “polishing stage” and this leads to a reduction in the cutting force. Figure 4(b) presents type 2 honing: this method corresponds to the use of two successive expansion speeds. For this type of cycle, expansion was started using a very powerful starting impulse. This programming tip on real machines allows the regulators to reduce the cycle time. This strong initial advance results in a faster increase in the cutting force and therefore allows removing more material. The stable abrasion cycle for the first expansion speed is reached at the 800th iteration. Switch from the first speed to the second is triggered by reaching an intermediate measurement before the final measurement. Reducing expansion speed disturbs cutting force, which is stable again at the 4500th iteration. Finally, reaching the zero measurement triggers the polishing stage. Here, polishing is maintained long enough for the cutting power and the roughness to both reach zero at the same time. Diagrams (figure 4) are comparable to the data coming from the monitoring of the Nagel VS8 MS-U4 honing machine.

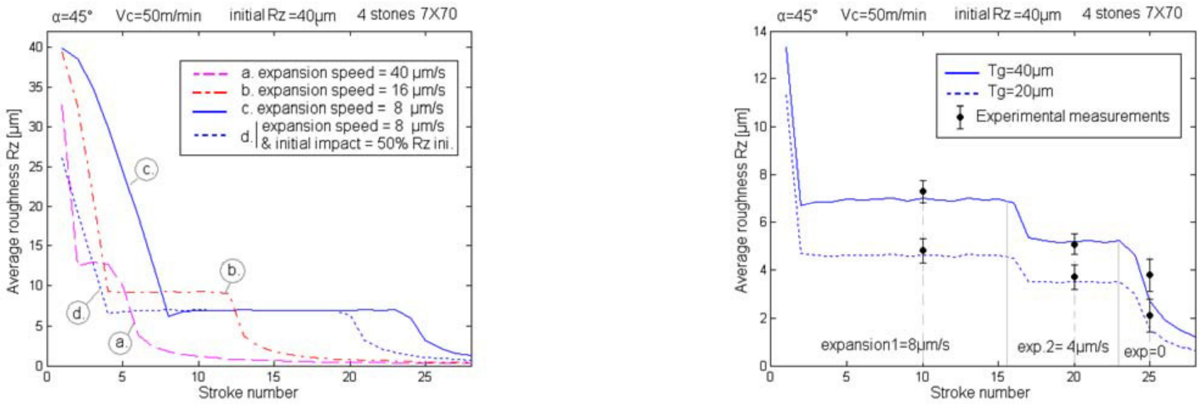

Fig. 5. Roughness evolution during the honing process, (a) Influence of expansion in type 1 cycle with IAS65/100 (*Tg*=40µm), (b) Influence of grit size and number of stones in type 2

3.2. Roughness obtained after abrasion

Thanks to the model of material removal after abrasion [13], the simulation allows one to observe local areas of roughness on each mesh during the honing cycle. The evolution of the mean roughness in the cylinder bore during the type 1 cycle was examined on a honing tool equipped with four stones using abrasives with an average grit indentation of 40 µm. The curves simulated for several constant expansion speeds are shown in Figure 5 (a) for abrasive stone IAS65/100. It is assumed that initial roughness is around 40 µm to better observe the decrease in roughness during the transitional cycle. It has been noticed that the stable cycle is reached more rapidly at an expansion speed of 16µm/s, but with the drawback of a roughness close to 9 µm. The final measurement, which triggers polishing, is obtained after 13 strokes whereas 23 are needed at an expansion speed of 8µm/s. An expansion speed of 8µm/s allows one to produce a roughness close to 7µm on a stabilized cycle. Starting the expansion via impulses is also simulated for an expansion speed of 8µm/s and one can observe that the stable regime is reached more rapidly and that consequently the cycle is shortened.

Figure 5 (b) represents the evolution of the mean roughness of the cylinder bore during the type 2 honing cycle for 2 abrasive stones whose average particle indentation is of 40 µm for the first stone, and 20 µm for the second. One can clearly identify the levels that correspond to the roughness produced on a stable regime. One can also note that the time constant is not affected by the grit size. A series of four cylinder bores (of the Renault K9K 1.5dCi engine) were honed according to the type 2 protocol, with two different abrasives. The maximum roughness of the honed cylinders was measured during the cycle after 10, 20 and 25 strokes. The points identified from these measurements are traced on Figure 5 (b). They confirm the validity of the abrasion model in stabilized cycles. The last measurement, after 25 strokes, is the furthest from the simulated roughness, because the phenomenon of abrasion during polishing is much too stochastic.

3.3. Surface aspect

Following a type 2 honing cycle with IAS65/100 abrasive stones, the prediction of texture quality leads to the results shown in figure 6. Mapping (a) allows one to observe that the visible final texture is composed of 50 to 100 traces made by the abrasive motion. Mapping (b) illustrates that, in general, the texture is composed by half of rising traces and by half of descending traces. Mapping (c) highlights total conformity in the middle of the cylinder bore. Non-compliant traces left by the abrasives during the periods of stroke motion inversion represent almost 20% of traces on the edges when the acceleration is worth 20 m/s².

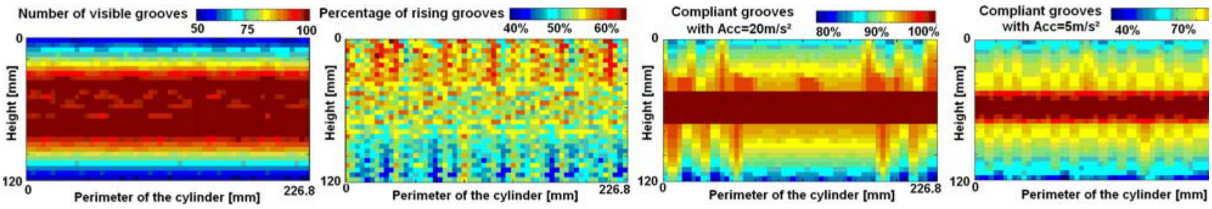

(a) (b) (c) (d)

Fig. 6. Mapping of surface aspect for 3 criteria

This phenomenon is even more visible when the acceleration is reduced to 5 m/s² as in figure 6(d). In this case, up to 70% of non-compliant grooves can be observed. In reality, it is easy to identify these non-compliant zones with the naked eye, by observing the interior surface under a well oriented light. The software allows one to predict these texture defects. At present only the eye of a specialist can describe such defects on a honed surface.

4. Conclusion

The honing simulation software presented in this article has been validated through experiment. It faithfully represents shape defects, roughness and gives accurate information about texture. The software allows one to predict the surface quality according to a maximum of process parameters. The impact of the kinematics on the roughness and texture has also been studied. This study has highlighted the fact that weak acceleration strongly deteriorates surface quality both during the simulation and in the experiment. In the lapping process, current cutting forces are very weak to limit the deformation of the cylinder. Consideration of more force requires the integration of macroscopic deformation of the piece. Knowledge of how surfaces are formed through abrasion is the first step in its tribological characterization. Digital surface models developed through honing simulation will be used shortly for a tribological study, which will allow linking functional surface performance with its production process.

References

[1] Santochi, M., Vignale, M., Giusti, F., 1982 A Study on the Functional Properties of a Honed Surface, CIRP Annals - Manufacturing Technology, 31/1:431-434.

[2] Haasis, G., Weigmann, U.-P., 1999, New honing technique reduces oil consumption, Industrial Diamond Review, Vol. 59, no. 582 pp. 205-210.

[3] Klocke, F., 2008, Manufacturing processes 2 - Grinding, Honing, Lapping, RWTHedi-tion.

[4] Ueda, T., Yamamoto, A., 1984, Analytical investigation of the honing mechanism, Journal of engineering for industry, 106 (3) pp. 237-241.

[5] Torrance, A.A., 2005, Modelling abrasive wear, Wear, 258 (1-4 SPEC. ISS.) pp. 281-293.

[6] Gouskov, A.M., Voronov, S.A., Butcher, E.A., Sinha, S.C., 2003, Influence of honing dynamics on surface formation, Pro-ceedings of the ASME Design Engineering Technical Conference, 5 C pp. 2239-2245.

[7] Voronov, S.A., Gouskov, A.M., Bobrenkov, O.A., 2009, Modeling of bore honing, International Journal of Mechatronics and Manufacturing Systems, 2 (5-6) pp. 566-579.

[8] Sabri, L., El Mansori, M., 2009, Process variability in honing of cylinder liner with vitrified bonded diamond tools, Surface and Coatings Technology, 204 (6-7) pp. 1046-1050.

[9] Ning, H., Li, X., Gong, J., Xu, H., 2011 Re-search on five sections measuring model in process pneumatic measurement system for inner hole honing, Advanced Materials Research, 317-319 pp. 1342-1346.

[10] Covington, P., Sabri, L., Le-Lan, J.V., Macroscopic cylinder honing process simulation, 12th CIRP Conference on Modeling of Machining Operations, Donostia-San-Sebastian, 7-8 May 2009.

[11] Tönshoff, H.K., Peters, J., Inasaki, I., Paul, T., 1992, Modeling and Simulation of Grinding Processes, CIRP Annals - Manufacturing Technology, 41/2:677-688.

[12] Szabó, O., 2004, Stability criteria and break out of grains of super-hard of grinding tools, Journal of Materials Processing Technology, 155-156 (1-3) pp. 2007-2010.

[13] Goeldel, B., El Mansori, M., Dumur, D., 2012, Macroscopic simulation of the liner honing process, CIRP Annals - Manufacturing Technology, vol. 61/1:319–322.

[14] International Organization for Standardization, Geneva, Switzerland, ISO 13565-2, Surface texture: profile method, surfaces having stratified functional properties, International Standard ISO, 1996.

[15] Buj Corral, I., Calvet, J.V., Salcedo, M.C., 2010 Use of roughness probability parameters to quantify the material removed in plateau-honing, International Journal of Machine Tools and Manufacture, 50 (7) pp. 621-629.

[16] El Mansori, M., Mezghani, S., Sabri, L., Zahouani, H., 2010, On the concept of process signature in analysis of multistage surface formation, Surface Engineering, Vol. 16, 3 pp. 216-223.

[17] Sabri, L., Mezghani, S., El Mansori, M., Zahouani, H., 2011, Multiscale study of finish-honing process in mass production of cylinder liner, Wear, 271 (3-4) pp. 509-513.

[18] Sabri, L., Mezghani, S., El Mansori, M., Le-Lan, J.V., 2009, Toward an objective 3D description for quality assessment of manufactured honed surfaces, Transactions of the North American Manufacturing Re-search Institution of SME, 37 pp. 661-668.